

Loop models on causal triangulations

Xavier Poncini

based on work with: Bergfinnur Durhuus, Jørgen Rasmussen and Meltem Ünel

PhD Candidate
University of Queensland

April 15, 2021



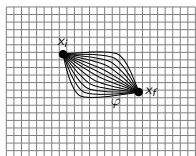
Outline

- 1 Motivation
- 2 Models
- 3 Tree correspondences
- 4 Transfer-matrix formalism
- 5 Critical behaviour
- 6 Conclusion



Path integral formulation

Quantum field theory admits a description in terms of the path integral:

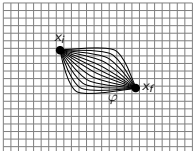


$$\longrightarrow \langle F \rangle = \int_{x_i \rightarrow x_f} \mathcal{D}\varphi F[\varphi] e^{iS[\varphi]}$$

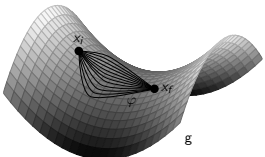


Path integral formulation

Quantum field theory admits a description in terms of the path integral:


$$\longrightarrow \langle F \rangle = \int_{x_i \rightarrow x_f} \mathcal{D}\varphi F[\varphi] e^{iS[\varphi]}$$

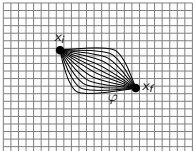
Constructing a naive quantum theory of gravity, let's just perform these calculations on a co-evolving background manifold:


$$\longrightarrow \langle F \rangle = \int_{x_i \rightarrow x_f} \mathcal{D}g \mathcal{D}\varphi F[g, \varphi] e^{iS[g, \varphi]}$$

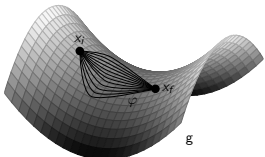


Path integral formulation

Quantum field theory admits a description in terms of the path integral:


$$\longrightarrow \langle F \rangle = \int_{x_i \rightarrow x_f} \mathcal{D}\varphi F[\varphi] e^{iS[\varphi]}$$

Constructing a naive quantum theory of gravity, let's just perform these calculations on a co-evolving background manifold:


$$\longrightarrow \langle F \rangle = \int_{x_i \rightarrow x_f} \mathcal{D}g \mathcal{D}\varphi F[g, \varphi] e^{iS[g, \varphi]}$$

Not generally renormalisable!

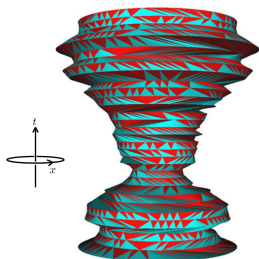


Causal dynamical triangulations

Causal dynamical triangulations (CDT) is an approach to quantum gravity that offers a reasonable way to compute the path integral:

$$\langle F \rangle = \int_{x_i \rightarrow x_f} \mathcal{D}g \mathcal{D}\varphi F[g, \varphi] e^{iS[g, \varphi]} \rightarrow \sum_{\mathcal{T}, \varphi} F[\mathcal{T}, \varphi] e^{iS[\mathcal{T}, \varphi]}$$

- 1 Define the manifold as a triangulation
- 2 Sum over all possible triangulations
- 3 Limit the volume of each simplex to zero

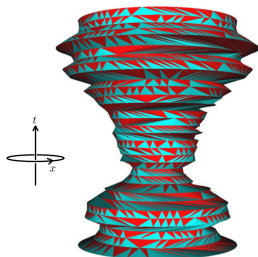


Causal dynamical triangulations

Causal dynamical triangulations (CDT) is an approach to quantum gravity that offers a reasonable way to compute the path integral

$$\langle F \rangle = \int_{x_i \rightarrow x_f} \mathcal{D}g \mathcal{D}\varphi F[g, \varphi] e^{iS[g, \varphi]} \rightarrow \sum_{T, \varphi} F[T, \varphi] e^{iS[T, \varphi]}$$

- 1 Define the manifold as a triangulation
- 2 Sum over all possible triangulations
- 3 Limit the volume of each simplex to zero



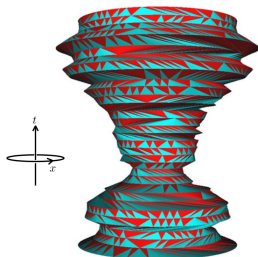
Causal dynamical triangulations

Causal dynamical triangulations (CDT) is an approach to quantum gravity that offers a reasonable way to compute the path integral

$$\langle F \rangle = \int_{x_i \rightarrow x_f} \mathcal{D}g \mathcal{D}\varphi F[g, \varphi] e^{iS[g, \varphi]} \rightarrow \sum_{T, \varphi} F[T, \varphi] e^{iS[T, \varphi]}$$

- 1 Define the manifold as a triangulation
- 2 Sum over all possible triangulations
- 3 Limit the volume of each simplex to zero

Work in progress!

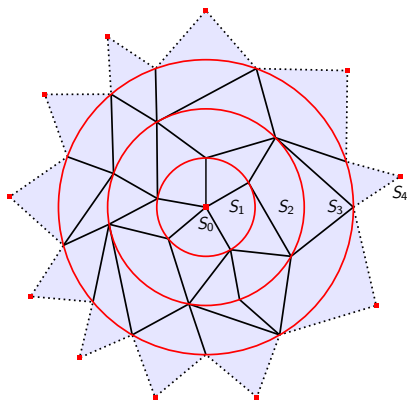


Models



Pure CDT model

A causal triangulation of a sphere is defined by a sequence of circular graphs (cycles) $S_0, S_1, \dots, S_m, S_{m+1}$, where $m \in \mathbb{N}$ is the height

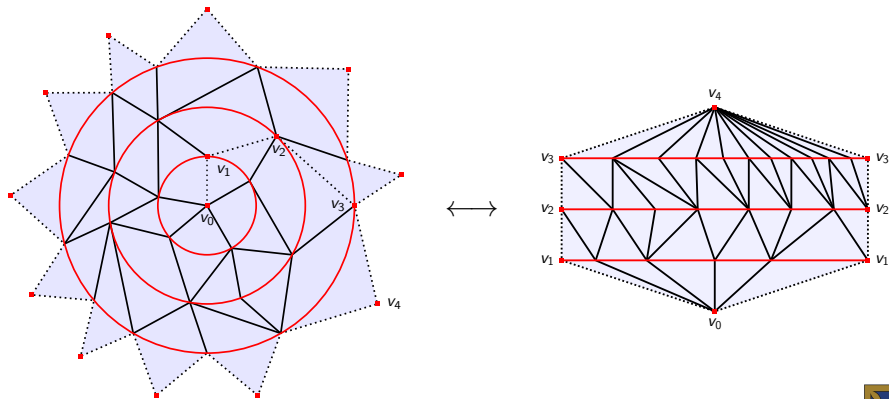


such that the annulus between two cycles is triangulated. Space-like edges are coloured red, while time-like edges are coloured black.



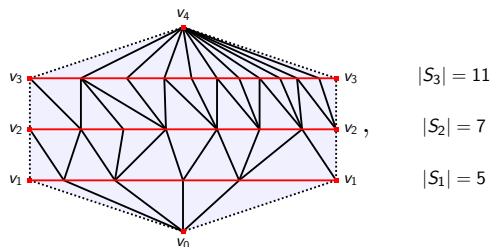
Pure CDT model

Each triangulation of the sphere admits a unique map to the plane defined by the sequence $v_0, v_1, \dots, v_m, v_{m+1}$:



Pure CDT model

For $C \in \mathcal{C}_m$, denote $|S_k|$ as the number of space-like edges per cycle and $|C| := \sum_{k=0}^m |S_k|$ the total number of space-like edges in C .



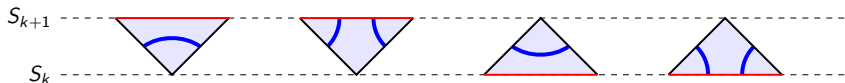
The pure CDT partition functions are:

$$Z^P(g) := \sum_{m=0}^{\infty} Z_m^P(g), \quad Z_m^P(g) := \sum_{C \in \mathcal{C}_m} g^{|C|}.$$

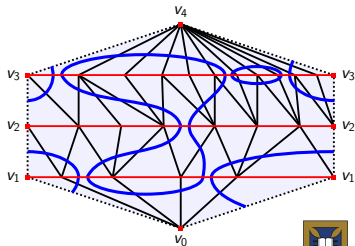
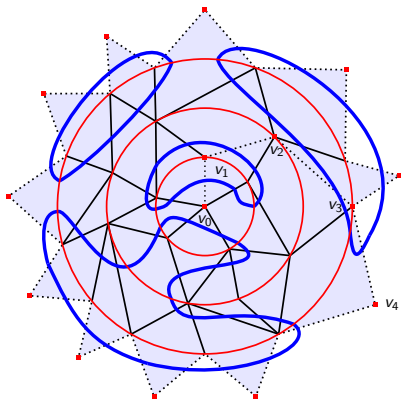


Dense loop model

Elementary triangles in each configuration $C \in \mathcal{C}_m$ are replaced with:

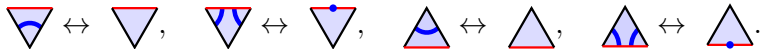


The resulting set of *dense loop model* configurations is denoted \mathcal{L}_m^{de} .

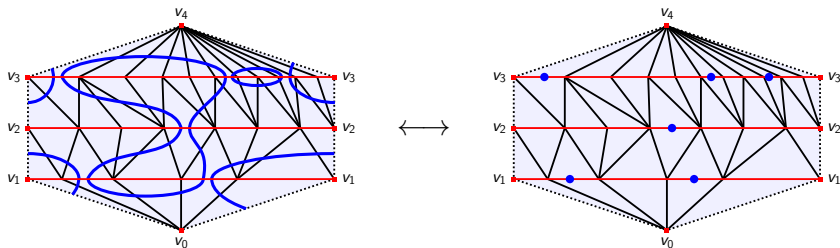


Dense loop model

Configurations of the dense loop model can be uniquely expressed by the *node* notation:



Returning to our previous example:

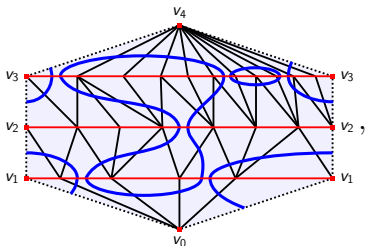


Each space-like edge can either be marked or unmarked.



Dense loop model

For $L \in \mathcal{L}_m^{de}$, denote $\ell(S_k)$ as the number of space-like edge intersections per cycle and $\ell(L) := \sum_{k=0}^{m+1} \ell(S_k)$ the total number of intersections in L .



$$|S_3| = 11, \quad \ell(S_3) = 6$$

$$|S_2| = 7, \quad \ell(S_2) = 2$$

$$|S_1| = 5, \quad \ell(S_1) = 4$$

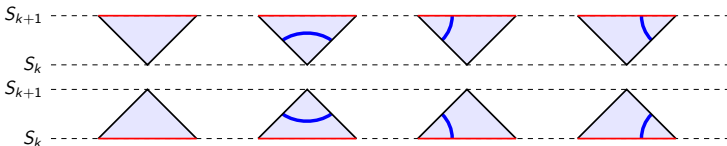
The dense loop model partition functions are:

$$Z^{de}(g, \alpha) := \sum_{m=0}^{\infty} Z_m^{de}(g, \alpha), \quad Z_m^{de}(g, \alpha) := \sum_{L \in \mathcal{L}_m^{de}} g^{|L|} \alpha^{\ell(L)}.$$

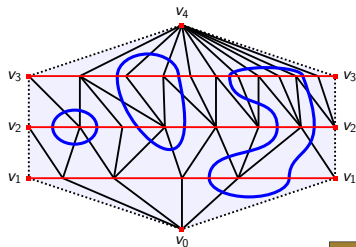
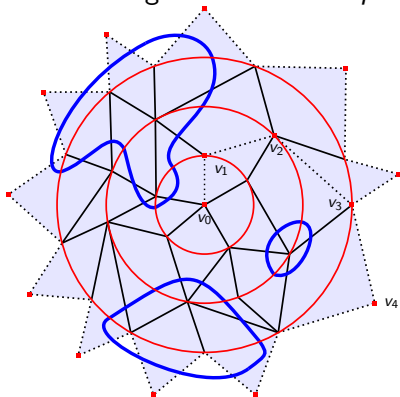


Dilute loop model

Elementary triangles in each configuration $C \in \mathcal{C}_m$ are replaced with:

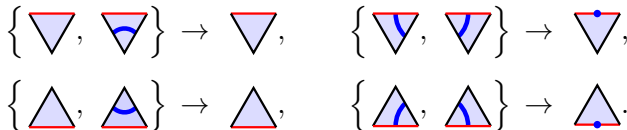


The resulting set of *dilute loop model* configurations is denoted \mathcal{L}_m^{di} .

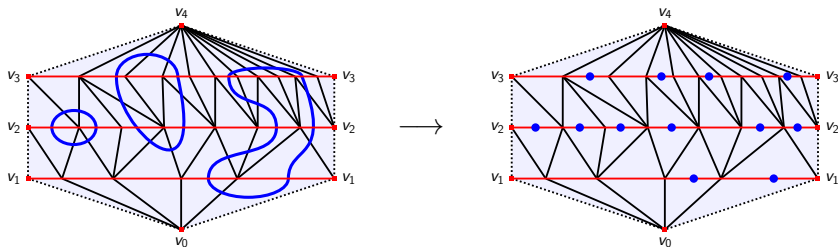


Dilute loop model

Configurations of the dilute loop model can be expressed using the *node* notation:



Returning to our previous example:

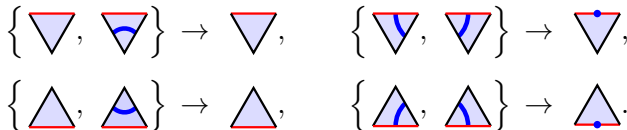


The loops are in 2^{m+1} to 1 correspondence with the nodes. There also exists a condition for nodes on each layer: $\#_k(\bullet) \in 2\mathbb{N}, 1 \leq k \leq m$.

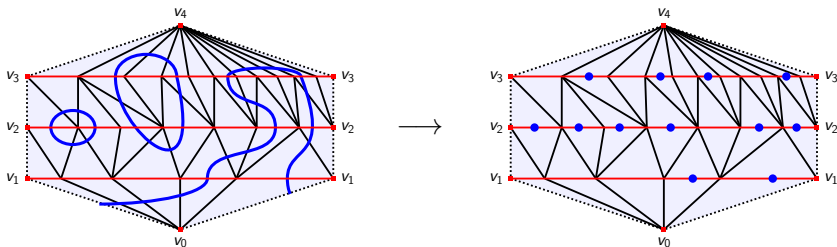


Dilute loop model

Configurations of the dilute loop model can be expressed using the *node* notation:



Returning to our previous example:

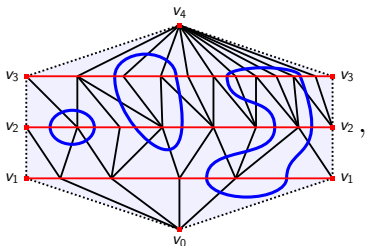


The loops are in 2^{m+1} to 1 correspondence with the nodes. There also exists a condition for nodes on each layer: $\#_k(\bullet) \in 2\mathbb{N}, 1 \leq k \leq m$.



Dilute loop model

For $L \in \mathcal{L}_m^{di}$, denote $\ell(S_k)$ as the number of space-like edge intersections per cycle and $\ell(L) := \sum_{k=0}^{m+1} \ell(S_k)$ the total number of intersections in L .



$$|S_3| = 11, \quad \ell(S_3) = 4$$

$$|S_2| = 7, \quad \ell(S_2) = 6$$

$$|S_1| = 5, \quad \ell(S_1) = 2$$

The dilute loop model partition functions are:

$$Z^{di}(g, \alpha) := \sum_{m=0}^{\infty} Z_m^{di}(g, \alpha), \quad Z_m^{di}(g, \alpha) := \sum_{L \in \mathcal{L}_m^{di}} g^{|L|} \alpha^{\ell(L)}.$$



Critical behaviour

Having defined partition functions relevant to each model. These objects need not be well defined over the entire parameter space of $g, \alpha \in \mathbb{C}$. That is there may exist a critical coupling g_c for each model such that

$$Z^P(g) = \begin{cases} \text{Convergent,} & |g| < g_c \\ \text{Critical point,} & g = g_c \\ \text{Divergent,} & g > g_c, \end{cases}$$

$$Z^*(g, \alpha) = \begin{cases} \text{Convergent,} & |g(\alpha)| < g_c(\alpha) \\ \text{Critical curve,} & g(\alpha) = g_c(\alpha) \\ \text{Divergent,} & g(\alpha) > g_c(\alpha), \end{cases}$$

where $\star \in \{de, di\}$. Determining the critical coupling allows one to establish the domain over which the model is well-defined.

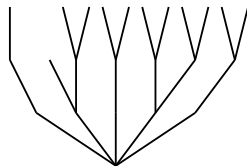


Tree correspondences



Planar trees

Let \mathcal{T}_m denote the set of height m planar trees. An example tree:



Denote $V_k(T)$ the set of vertices of $T \in \mathcal{T}_m$ with distance k from root and $V(T)$ the vertex set of T excluding the root

$$V(T) := \bigcup_{k=1}^m V_k(T).$$

Note that $V(T)$ is equal to the number of edges in T .

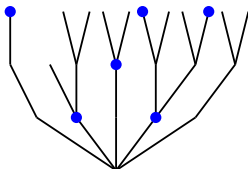


Labelled Planar trees

Let $\tilde{\mathcal{T}}_m$ denote the set of height m labelled planar trees

$$\tilde{\mathcal{T}}_m := \{(T, \delta) \mid T \in \mathcal{T}_m, \delta : V(T) \rightarrow \{0, 1\}\},$$

an example:



We define the *labelling characteristics*

$$|\delta| := \sum_{k=1}^m \delta_k, \quad \delta_k := \sum_{v \in V_k(T)} \delta(v), \quad k = 1, \dots, m,$$

and the restricted set of labelled trees

$$\tilde{\mathcal{T}}_m^{ev} := \{(T, \delta) \in \tilde{\mathcal{T}}_m \mid \delta_k \in 2\mathbb{N}_0, k = 1, \dots, m\}.$$



Tree partition functions

To each set of trees \mathcal{T}_m , $\tilde{\mathcal{T}}_m$ and $\tilde{\mathcal{T}}_m^{ev}$, we associate the partition functions

$$W(g) := \sum_{m=0}^{\infty} W_m(g), \quad W_m(g) := \sum_{T \in \mathcal{T}_m} g^{V(T)},$$

$$W(g, \alpha) := \sum_{m=0}^{\infty} W_m(g, \alpha), \quad W_m(g, \alpha) := \sum_{(T, \delta) \in \tilde{\mathcal{T}}_m} g^{V(T)} \alpha^{|\delta|},$$

$$W^{ev}(g, \alpha) := \sum_{m=0}^{\infty} W_m^{ev}(g, \alpha), \quad W_m^{ev}(g, \alpha) := \sum_{(T, \delta) \in \tilde{\mathcal{T}}_m^{ev}} g^{V(T)} \alpha^{|\delta|},$$

recall $V(T)$ count edges of a tree T , $|\delta|$ count the number of 1 labels.

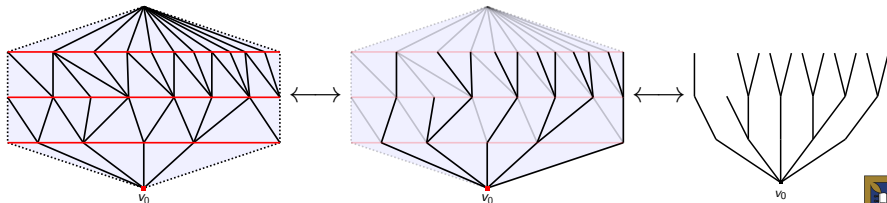


Pure CDT model bijection

There exists a bijective correspondence between triangulations and trees:

$$\psi : \mathcal{C}_m \rightarrow \mathcal{T}_m$$

- Remove all space-like (red) edges
- For each vertex, remove the leftmost outward-pointing time-like (black) edge

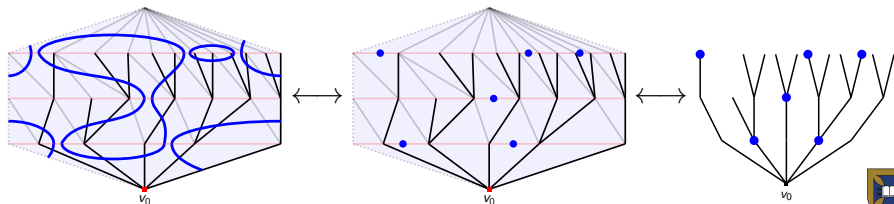


Dense loop model bijection

There exists a bijective correspondence between triangulations and trees:

$$\tilde{\psi} : \mathcal{L}_m^{de} \rightarrow \tilde{\mathcal{T}}_m$$

- Remove all space-like (red) edges
- For each vertex, remove the leftmost outward-pointing time-like (black) edge
- Label each vertex to the right of an intersected space-like edge

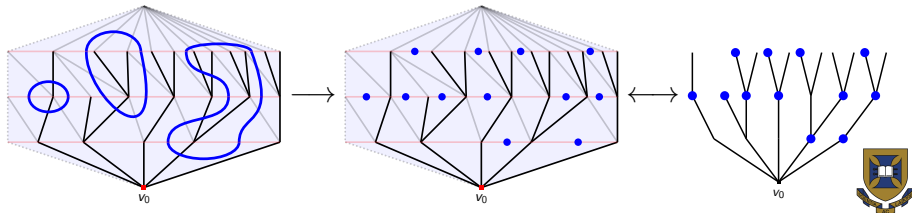


Dilute loop model correspondence

There exists a 2^{m+1} to 1 correspondence between triangulations and trees:

$$\hat{\psi} : \mathcal{L}_m^{di} \rightarrow \tilde{\mathcal{T}}_m^{ev}$$

- Remove all space-like (red) edges
- For each vertex, remove the leftmost outward-pointing time-like (black) edge
- Label each vertex to the right of an intersected space-like edge



Relating partition functions

- Causal triangulations and planar trees:

$$Z^P(g) = W(g)$$

- Dense loop causal triangulations and labelled planar trees:

$$Z^{de}(g, \alpha) = W(g, \alpha^2)$$

- Dilute loop causal triangulations and even labelled planar trees:

$$Z^{di}(g, \alpha) = 1 + \sum_{m=1}^{\infty} 2^{m+1} W_m^{ev}(g, \alpha)$$

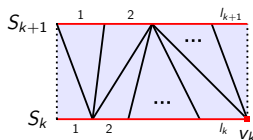


Transfer-matrix formalism



Preliminary result

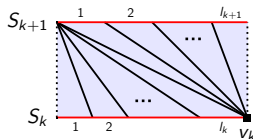
Consider an arbitrary triangulation A_k of a single time-slice with boundary lengths $l_k \equiv |S_k|$ and $l_{k+1} \equiv |S_{k+1}|$:



applying a sequence of local flips



A_k can be transformed into any other triangulation possessing boundary lengths l_k and l_{k+1} . In particular the *standard triangulation*:

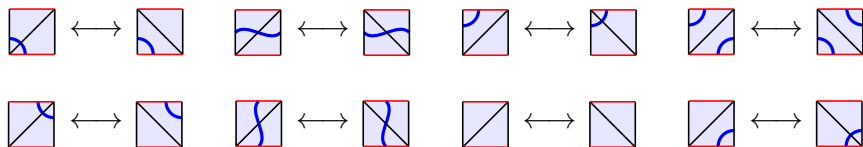


Preliminary result

Extending the flip operation to the dense model



and the dilute model



It follows:

- (i) The number of possible dense/dilute, loop configurations on a single time-slice only depends on the boundary lengths l_k and l_{k+1} .
- (ii) The flip operations applied to a loop configuration leave the number of space-like edges and intersections invariant.

Consequently, the details of the triangulation decouple from the loop configurations.



Transfer-matrix

We denote the combinatorial operator generating all infinitesimal configurations as the transfer-matrix, whose elements are given by:

$$T_{d,u}^* := \sum_{d_i, u_i} \text{Coeff}_* \left(\text{Diagram} \right) = \binom{d+u-1}{u} \text{Coeff}_* \left(\text{Diagram} \right),$$

The first diagram is a long blue triangle with a red base and a red top edge, divided into smaller triangles by dashed lines. The bottom edge is labeled with $d_1, u_1, d_2, u_2, \dots$. The second diagram is a smaller blue triangle with a red base and a red top edge, divided into smaller triangles by dashed lines. The bottom edge is labeled d and the top edge is labeled u .

where $\star \in \{p, de, di\}$, the binomial coefficient counts distinct triangulations possessing $d = \sum_{i=1}^n d_i$ lower and $u = \sum_{i=1}^n u_i$ upper space-like edges, Coeff_\star counts weights associated with the expansions:

$$\begin{aligned}
 p &: \triangle := g \triangle \\
 de &: \triangle := g \left(\triangle + \alpha \triangle \right) \\
 di &: \triangle := g \left(\triangle + \triangle + \alpha^{\frac{1}{2}} \left[\triangle + \triangle \right] \right)
 \end{aligned}$$

The diagrams in the expansions show blue arcs on the edges of the triangles, representing different types of configurations.



Transfer matrix

$$T_{d,u}^{\star} = \binom{d+u-1}{u} \text{Coeff}_{\star} \left(\begin{array}{c} u \\ \text{---} \\ \text{---} \\ \text{---} \\ \text{---} \\ \text{---} \\ \text{---} \\ \text{---} \\ \text{---} \\ d \end{array} \right),$$

Expanding the coefficient for each $\star \in \{p, de, di\}$

$$T_{d,u}^p = \binom{d+u-1}{u} g^{\frac{d+u}{2}}$$

$$T_{d,u}^{de} = \binom{d+u-1}{u} (g(1+\alpha^2))^{\frac{d+u}{2}}$$

$$T_{d,u}^{di} = \binom{d+u-1}{u} [(g(1+\alpha))^d + (g(1-\alpha))^d]^{\frac{1}{2}} [(g(1+\alpha))^u + (g(1-\alpha))^u]^{\frac{1}{2}}$$



Transfer matrix

Defining the vectors relevant to each model $\star \in \{p, de, di\}$, the k^{th} components of $|v^{\star}(g, \alpha)\rangle$ and $\langle v^{\star}(g, \alpha)|$, are

$$|v_k^{\star}(g, \alpha)\rangle := \text{Coeff}_{\star} \left(\begin{array}{c} \text{---} \\ \backslash \\ \text{---} \\ \text{---} \\ \backslash \\ \text{---} \end{array} \right)_k, \quad \langle v_k^{\star}(g, \alpha)| := \text{Coeff}_{\star} \left(\begin{array}{c} \text{---} \\ / \\ \text{---} \\ \text{---} \\ / \\ \text{---} \end{array} \right)_k.$$

The m height partition function of each model can be written

$$Z_m^{\star}(g, \alpha) = \langle v^{\star}(g, \alpha) | \mathcal{T}^{\star m-1} | v^{\star}(g, \alpha) \rangle.$$

Diagrammatically this corresponds to

$$Z_m^{\star}(g, \alpha) = \sum_{d_i^k, u_i^k} \vec{\delta}_u^d \text{Coeff}_{\star} \left(\begin{array}{c} \text{---} \\ \backslash \\ \text{---} \\ \text{---} \\ \backslash \\ \text{---} \\ \vdots \\ \text{---} \\ \text{---} \\ \backslash \\ \text{---} \\ \text{---} \\ \backslash \\ \text{---} \\ \vdots \\ \text{---} \\ \text{---} \\ \backslash \\ \text{---} \\ \text{---} \\ \backslash \\ \text{---} \\ \text{---} \\ \backslash \\ \text{---} \\ \text{---} \\ \backslash \\ \text{---} \\ \text{---} \\ \backslash \\ \text{---} \\ \text{---} \\ \backslash \\ \text{---} \end{array} \right), \quad \text{where } \vec{\delta}_u^d := \prod_{i=0}^m \delta_{u_i}^{d_{i+1}}.$$



Critical behaviour



Pure CDT model

The planar tree partition function admits the recursion and solution

$$W(g) = \frac{1}{1 - gW(g)}, \quad W(g) = \frac{1 - \sqrt{1 - 4g}}{2g}.$$

Given the relation

$$Z^P(g) = W(g), \quad \mathbb{D} = \{g \in \mathbb{C} \mid |g| < \frac{1}{4}\},$$

it follows that the pure CDT model is analytic on the disk \mathbb{D} with $g_c = \frac{1}{4}$. The partition function admits an expansion

$$Z^P(g) = 2 \sum_{n=0}^{\infty} (-1)^n \left(\frac{g_c - g}{g_c} \right)^{\frac{n}{2}},$$

and consequently has a critical exponent of $\frac{1}{2}$. With the Hausdorff dimension shown to be 2 almost surely, Durhuus et. al. (2010).



Dense loop model

Evaluating the summation over labels δ

$$W_m(g, \alpha) = \sum_{(T, \delta) \in \tilde{\mathcal{T}}_m} g^{V(T)} \alpha^{|\delta|} = \sum_{T \in \mathcal{T}_m} (g(1 + \alpha))^{V(T)} = W_m(g(1 + \alpha)).$$

Recalling

$$Z^{de}(g, \alpha) = W(g, \alpha^2), \quad Z^P(g) = W(g),$$

the pure CDT partition function is equal to the dense partition function under the shift in coupling $g \rightarrow g(1 + \alpha^2)$. It follows that the dense loop model is analytic on the disk

$$\mathbb{D}_{\alpha^2} = \left\{ (g, \alpha^2) \in \mathbb{C}^2 \mid |g| < \frac{1}{4(1 + |\alpha^2|)} \right\},$$

and possesses the same critical exponent of $\frac{1}{2}$.



Evaluating the summation over labels δ

$$W_m^{ev}(g, \alpha) = \sum_{(T, \delta) \in \tilde{\mathcal{T}}_m^{ev}} g^{V(T)} \alpha^{|\delta|} = \sum_{T \in \mathcal{T}_m} g^{V(T)} \prod_{i=0}^m \frac{1}{2} [(1 + \alpha)^{V_i(T)} + (1 - \alpha)^{V_i(T)}].$$

Recalling

$$Z^{di}(g, \alpha) = \sum_{m=0}^{\infty} 2^{m+1} W_m^{ev}(g, \alpha).$$

Unlike the previous case, this partition function cannot be interpreted as a simple shift to the coupling of the pure CDT partition function.

Determining the critical behaviour we turn to the transfer matrix.



Dilute loop model

Expressing the partition function in terms of the transfer matrix

$$Z^{di}(g, \alpha) = 1 + \sum_{m=1}^{\infty} \langle v^{di}(g, \alpha) | (T^{di}(g, \alpha))^{m-1} | v^{di}(g, \alpha) \rangle.$$

The operator T^{di} admits the factorisation

$$T^{di}(g, \alpha) = 2DK^{di}(g, \alpha),$$

where

$$D_{r,s} = \frac{\delta_{r,s}}{r},$$

$$K_{r,s}^{di}(g, \alpha) = \frac{1}{2} \frac{(r+s-1)!}{(r-1)!(s-1)!} [(1+\alpha)^r + (1-\alpha)^r]^{\frac{1}{2}} [(1+\alpha)^s + (1-\alpha)^s]^{\frac{1}{2}} g^{\frac{r+s}{2}}.$$

The partition function can be re-expressed as

$$Z^{di}(g, \alpha) = 1 + \sum_{m=1}^{\infty} \langle v | D^{\frac{1}{2}} (2D^{\frac{1}{2}} K^{di} D^{\frac{1}{2}})^{m-1} D^{-\frac{1}{2}} | v \rangle.$$



Various facts:

The operator $D^{\frac{1}{2}} K^{di} D^{\frac{1}{2}}$ is analytic on the disk

$$\mathbb{D}_\alpha = \left\{ (g, \alpha) \in \mathbb{C}^2 \mid |g| < \frac{1}{4(1+|\alpha|)} \right\},$$

possessing an orthonormal set of eigenvectors $\{|w^{(m)}(g, \alpha)\rangle \mid m \in \mathbb{N}\}$ and a corresponding set of eigenvalues $\{\lambda_m(g, \alpha) \mid m \in \mathbb{N}\}$. There exists a largest eigenvalue $\lambda_1(g, \alpha)$ that is an increasing function of g . Defining

$$\bar{\lambda}_1(\alpha) := \lim_{g \nearrow \frac{1}{4(1+\alpha)}} \lambda_1(g, \alpha),$$

the endpoints of $\bar{\lambda}_1(\alpha)$ over $\alpha \in [0, 1]$ are given by

$$\bar{\lambda}_1(0) = 1, \quad \bar{\lambda}_1(1) = \frac{1}{2}.$$



These facts facilitate the following calculation:

$$\begin{aligned}
 Z^{di}(g, \alpha) - 1 &= \sum_{m=1}^{\infty} \langle v | D^{\frac{1}{2}} (2D^{\frac{1}{2}} K^{di} D^{\frac{1}{2}})^{m-1} D^{-\frac{1}{2}} | v \rangle \\
 &= \sum_{m,n=1}^{\infty} \langle v | D^{\frac{1}{2}} (2D^{\frac{1}{2}} K^{di} D^{\frac{1}{2}})^{m-1} | w^{(n)} \rangle \langle w^{(n)} | D^{-\frac{1}{2}} | v \rangle \\
 &= \sum_{m,n=1}^{\infty} (2\lambda_n)^{m-1} \langle v | D^{\frac{1}{2}} | w^{(n)} \rangle \langle w^{(n)} | D^{-\frac{1}{2}} | v \rangle \\
 &= \sum_{n=1}^{\infty} \frac{\langle v | D^{\frac{1}{2}} | w^{(n)} \rangle \langle w^{(n)} | D^{-\frac{1}{2}} | v \rangle}{1 - 2\lambda_n} \\
 &\geq \frac{c^2}{1 - 2\lambda_1} - \frac{\|D^{\frac{1}{2}} v\| \|D^{-\frac{1}{2}} v\|}{1 - 2\lambda_2}
 \end{aligned}$$

where we run into trouble for $\lambda_1(g, \alpha) = \frac{1}{2}$!



Dilute loop model

Selecting a sufficiently small α such that $\bar{\lambda}_1(\alpha) > \frac{1}{2}$ the critical coupling of the dilute loop model $g_c^{di}(\alpha)$ is uniquely given by the equation

$$\lambda_1(g_c^{di}(\alpha), \alpha) = \frac{1}{2}, \quad \text{where } g_c^{di}(\alpha) < \frac{1}{4(1+\alpha)}.$$

Consider an $0 < \alpha \leq 1$ such that $\bar{\lambda}_1(\alpha) = \frac{1}{2}$, the above arguments break down as it implies

$$g_c^{di}(\alpha) = \frac{1}{4(1+\alpha)}, \quad g_c^{di}(\alpha) \notin \mathbb{D}_\alpha.$$

Thus we have the two possibilities

- (i) $\bar{\lambda}_1(\alpha) = \frac{1}{2}$ for $\alpha = 1$, the constraint holds for all $\alpha \in [0, 1]$.
- (ii) $\bar{\lambda}_1(\alpha) = \frac{1}{2}$ for $\alpha \in [\alpha_0, 1]$ $\alpha_0 < 1$, suggesting a phase transition.



Dilute loop model

Let us now consider the critical exponent of the dilute loop model. From the previous lower bound we can conclude for g close to $g_c^{di}(\alpha)$, we have

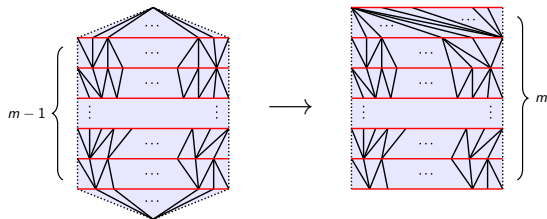
$$\frac{C_1(\alpha)}{g_c^{di}(\alpha) - g} \leq Z^{di}(g, \alpha).$$

Establishing an upper bound we define

$$Z_m^{per}(g, \alpha) := \text{tr}(T^{di}(g, \alpha))^{m-1}, \quad m \geq 2$$

and identify the inequality

$$Z_m^{di}(g, \alpha) \leq 2Z_{m+1}^{per}(g, \alpha), \quad m \geq 1$$



Dilute loop model

Applying the inequality

$$Z_m^{di}(g, \alpha) \leq 2Z_{m+1}^{per}(g, \alpha) \leq 2(\text{tr } T^{di}(g, \alpha))^m,$$

to the full partition function

$$Z^{di}(g, \alpha) \leq 1 + \sum_{m=1}^{\infty} 2^{m+1} (\text{tr } D^{\frac{1}{2}} K^{di}(g, \alpha) D^{\frac{1}{2}})^m = 1 + \sum_{n=1}^{\infty} \frac{4\lambda_n(g, \alpha)}{1 - 2\lambda_n(g, \alpha)},$$

we have an upper bound for the partition function for g close to $g_c^{di}(\alpha)$

$$\frac{C_1(\alpha)}{g_c^{di}(\alpha) - g} \leq Z^{di}(g, \alpha) \leq \frac{C_2(\alpha)}{g_c^{di}(\alpha) - g}.$$

It follows that for α small, the critical exponent of the dilute loop model is -1 ! Inducing a shift from $\frac{1}{2}$ of the pure CDT model.

Accompanying this shift is a change in Hausdorff dimension from 2 to 1, Durhuus and Ünel (2021).



Conclusion



Conclusion

Take home points:

- Pure CDT and dense loop models possess identical critical behaviour
- For α small, the critical behaviour of the dilute loop model is distinct from pure CDT suggesting a non-trivial loop-triangulation coupling
- This coupling induces a change in Hausdorff dimension from 2 to 1

Future direction:

- Examine $\bar{\lambda}_1(\alpha)$ further to investigate the presence of α_0
- Analyse a generalisation of the dilute model where we introduce a new parameter γ as follows:

$$\triangle := g \left(\triangle + \gamma^{\frac{1}{2}} \triangle + \alpha^{\frac{1}{2}} \left[\triangle + \triangle \right] \right)$$

- Consider other loop models on triangulations incorporating a braid e.g the BMW algebra

